Journal of Molecular Catalysis A: Chemical 346 (2011) 46–54

Contents lists available at ScienceDirect

Journal of Molecular Catalysis A: Chemical

journal homepage: www.elsevier.com/locate/molcata

Acid–base properties of the active sites responsible for C_2^+ and CO_2 formation over MO–Sm_2O_3 (M = Zn, Mg, Ca and Sr) mixed oxides in OCM reaction

Florica Papa[a], Patron Luminita[a], Petre Osiceanu[a], Ruxandra Birjega[b], Miyazaki Akane[c], Ioan Balint[a,*]

[a] Institute of Physical Chemistry of the Romanian Academy, Spl. Independentei 202, 060021 Bucharest, Romania
[b] National Institute for Lasers, Plasma and Radiation Physics Lasers Department 409 Atomistilor, PO Box MG-16, 077125 Magurele-Bucharest, Romania
[c] Department of Chemical and Biological Sciences, Faculty of Science, Japan Women's University, 2-8-1 Mejirodai, Bunkyo-ku, Tokyo 112-8681, Japan

ARTICLE INFO

Article history:
Received 1 April 2011
Received in revised form 20 June 2011
Accepted 21 June 2011
Available online 28 June 2011

Keywords:
Oxidative coupling of methane
Methane oxidative conversion
Oxide surface basicity
Lanthanide-alkaline-earth oxides catalysts

ABSTRACT

The research investigates the quantitative relationship between the surface basicity of MO–Sm_2O_3 (M = Zn, Mg, Ca and Sr) mixed oxides and catalytic activity for C_2^+ formation. The amount as well as the evolution of surface carbonate species with nature of MO and reaction temperature were analyzed by XRD, TPD, XPS and IR methods to better understand the reaction mechanism. The concentration of surface basic sites responsible for the formation of C_2^+ were found to correlate well with the amount of evolved CO_2 in the 300–800 °C temperature range. According to the experimental data, the higher was the catalyst basicity in terms of CO_2 retaining capacity the better was the efficiency for selectively converting methane to C_2^+. The turnover frequency (TOF) values were calculated by measuring the total number basic sites retaining reversible CO_2 in reaction conditions. The experimental results can be explained in a simplified manner by considering a reaction mechanism in which alkaline active sites play a crucial role in methane selective activation to C_2^+ whereas the acidic sites, showing little interaction CO_2, are responsible for methane combustion. A strategy for improving the performances of OCM catalysts is discussed in light of the experimental results.

1. Introduction

Methane is still an abundant and relatively cheap natural resource. One versatile way for better utilization of methane is the catalytic oxidative conversion to obtain either energy (i.e. low-temperature combustion in gas turbines) or added value products such as higher hydrocarbons (C_xH_y), CO, H_2 and oxygenated products. Methane oxidative coupling (OCM) is a convenient way for the synthesis of ethane and ethylene via one step reaction. This reaction attracted considerable attention over decades due its high economic potential. Among the large number of oxides and mixed oxides tested, the best performances were obtained over the basic oxide compounds. Theoretical calculations predict that the upper bound yield to C_2^+ is below 30% [1]. On the other hand, from economical point of view the yield to C_2^+ should overpass the 30% limit. One of the main drawbacks of OCM reaction is not only low production of C_2^+ but the formation of large amounts of CO_2 which is the unselective reaction product of methane oxidation. In order to improve the catalysts performances, extensive studies for the identification of the sites responsible for methane selective activation have been performed. The conclusion is somehow puzzling as several possible active sites have been proposed, depending on the catalytic materials used. The active sites considered responsible for methane selective activation to $CH_3^\bullet$ radicals by the extraction of one hydrogen atom were O^-, O_2^- and O_2^{2-} oxygen species. A clear and generally accepted conclusion concerning the nature of active sites as well as the quantitative relationship existing between these sites, the basic properties of the catalytic materials and the catalytic behavior in OCM reaction was not drawn yet. However, the above mentioned lattice oxygen species must have more or less basic properties in order to activate selectively methane and these sites should be generated under reaction conditions. In a recently published work, the contribution of acid and basic sites of MO–Nd_2O_3 (M = Be, Mg, Ca, Sr) mixed to the oxidative conversion of methane was investigated in details [2]. This work is among the first attempts aiming to demonstrate that the methane conversion over oxide catalysts can be well understood if it is interpreted in simple terms of acid–base catalysis. The acid–base properties of the catalytic materials were systematically modified by adding to Sm_2O_3 equimolecular amounts of alkaline-earth oxides (MgO, CaO and SrO). In addition, the influence of ZnO, known as having amphoteric characteristics, on the catalytic behavior of Sm_2O_3 was also investigated. The interpretation of catalytic results in terms of acid–base theory is intended to help the understanding of reaction mechanism, allowing thus to find effective ways to improve the catalytic performances. The goals of the present research are

* Corresponding author. Tel.: +40 21224889; fax: +40 213121147.
E-mail address: ibalint@icf.ro (I. Balint).

1381-1169/$ – see front matter © 2011 Elsevier B.V. All rights reserved.
doi:10.1016/j.molcata.2011.06.008

to demonstrate that (i) the catalytic activity for C_2^+ formation is directly related to the overall basicity of catalysts (number of basic sites), and (ii) methane is oxidized to CO_2 on the acid sites.

2. Experimental

The MO–Sm_2O_3 (M = Zn, Mg, Ca, Sr) mixed oxides were prepared starting from the tartarate complexes of the constituent metals. The tartarate route favors the mixing of the components at molecular level. The complex precursors were synthesized by separately dissolving stoichiometric amounts of metal nitrates and tartaric acid in one to four molar ratio in minimum amounts of distilled water followed by the mixing of the resulted solutions. The solutions of complex metal tartarates were heated slowly to 80 °C then kept at this temperature for 1 h. After cooling to room temperature, ethanol was added and the pH was increased by addition of ammonium hydroxide (30%) in ethanol (1:1). The resulted light-yellow precipitates were maintained in liquid phase at 4 °C for 24 h, filtered, washed several times with pure ethanol and finally dried on P_4O_{10}. In all cases, the general formula of the insoluble heteropolynuclear complexes was $(NH_4)_x[MSm_2(Ta)_4(OH)_x]\cdot H_2O$ (M = Zn, Mg, Ca, Sr). The formulas were determined by atomic absorption spectroscopy and by gravimetric techniques. The C, N and H concentrations were measured with Carbo Erba Model 1108 CHNSO elemental analyzer. The final step consisted in the calcination of the complex precipitates at 800 °C for 2 h.

Activity tests for OCM reaction were performed at atmospheric pressure with 0.1 g of catalyst (0.3–0.8 mm fraction) loaded in a tubular quartz microreactor (i.d. = 8 mm). The blank tests with the reactor containing only quartz wool confirmed that the homogeneous conversion of CH_4 started from T >850 °C. The reactor was heated with a furnace connected to a temperature controller (Shimaden, Model SR 25). The reactant gaseous mixtures were prepared using electronic flow controllers (Aalborg and Kofloc). The 1% nitrogen in reactant mixture was used as internal reference. The typical total flow rate of the reaction mixture was 24 $cm^3\ min^{-1}$ STP (standard temperature and pressure) and the corresponding GHSV (gas hourly space velocity) was 14,400 h^{-1}. The composition of reaction mixture was 41.6% CH_4, 8.4% O_2 (CH_4/O_2 = 5/1) and balance Ar. The gaseous mixtures to and from the reactor were analyzed with a Buck Scientific gas chromatograph equipped with TCD detectors. The O_2, CH_4 were separated on a molecular sieve 13× column whereas CO_2, C_2H_6 and C_2H_4 separated on a Haysept column. Carbon balance was better than 95% in all cases. The catalytic behavior is expressed in terms of well-known methane conversion, selectivity and yields to C_2^+.

The crystalline structure of the prepared samples was analyzed with a Rigaku Multiflex diffractometer provided with peak assignment software using Cu Kα radiation (λ = 1.54 Å). All the diffraction patterns were recorded in 2θ range of 20–80° by a scanning rate of 2° min^{-1}.

Temperature programmed desorption (TPD) experiments with 0.1 g of catalyst were carried out in a flow system with a Chembet 3000-Quantachrome Instruments apparatus equipped with thermal conductivity detectors (TCD). The flow rate of Ar carrier gas was 70 ml min^{-1} and the typical heating rate of the catalysts was 10 °C min^{-1}. A silicagel water trap was interposed between the analyzed samples and the TCD detector in order to remove water vapors and thus to ensure good stability and sensitivity of the detection system. A mass spectrometer attached to the outlet confirmed that the measured desorbed specie was only CO_2.

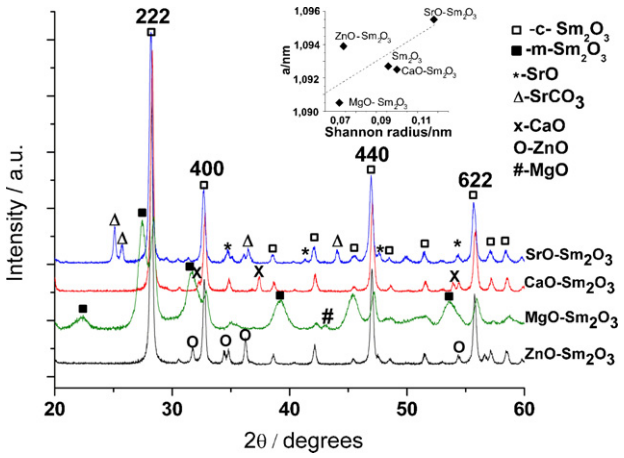

Fig. 1. Comparative XRD patterns of MO–Sm_2O_3 (M = Zn, Mg, Ca, Sr) mixed oxides. The inset presents the variation of lattice parameter (a) of the cubic Sm_2O_3 with the Schannon radius of M^{2+} ions.

The IR spectra were recorded in the 4000–400 cm^{-1} range with JASCO FT-IR 4100 spectrometer. Prior the measurements the oxide samples were homogenized with KBr using an agate mortar and then pressed in thin, transparent pellets.

The chemical formulas of the tartarate compound precursors were determined by atomic absorption spectroscopy and gravimetric techniques. The C, N and H concentrations were measured with Carbo Erba Model 1108 CHNSO elemental analyzer.

The surface composition was analyzed by X-ray Photoelectron Spectroscopy (XPS). The XPS data were acquired at 10^{-7} Pa using a VG K-Alpha spectrometer. The X-ray source was monochromatized AlKα radiation (1486.7 eV) and the overall energy resolution is estimated to be 0.45 eV.

3. Results and discussion

From the analysis data, consistent with the chemical formulas presented in Table 1, it is clear that the initial stoichiometry is preserved during the synthesis process.

3.1. XRD analysis

The XRD patterns of the investigated catalytic oxide mixtures are presented in Fig. 1. According to XRD data the presence of alkaline-earth oxides favored the formation of a well-crystallized cubic structure for Sm_2O_3 (JCPDS file 15-813). The cubic lattice parameters as well as the Scherrer crystallite sizes of the simple, ZnO or alkaline-earth oxide added Sm_2O_3 are listed in Table 2. In the case of solid solution formation it can be assumed that the

Table 1
Elemental analysis.

Formula calculated from the elemental analysis data	M[a]/wt%	Sm/wt%	N/wt%	C/wt%	H/wt%
$(NH_4)_2[ZnSm_2(C_4O_6H_4)_4(OH)_2]\cdot 6H_2O$	5.45	25.24	1.81	16.52	3.1
$(NH_4)_5[MgSm_2(C_4O_6H_4)_4(OH)_5]\cdot 6H_2O$	2.06	25.82	6.28	15.62	3.62
$(NH_4)[CaSm_2(C_4O_6H_4)_4(OH)]\cdot 7H_2O$	3.66	27.56	1.48	17.02	3.44
$(NH_4)_2[SrSm_2(C_4O_6H_4)_4(OH)_2]\cdot 6H_2O$	7.22	24.80	2.42	16.05	3.16

[a] M = alkaline-earth elements (Mg, Ca, Sr, Zn).

Table 2
Lattice parameters (a) and crystallite size (D) of MO–Sm_2O_3 mixed oxides.

Sample	*a*/Å	*D*/nm
ZnO–Sm_2O_3	10.939	46
MgO–Sm_2O_3	10.905	20
CaO–Sm_2O_3	10.925	39
SrO–Sm_2O_3	10.955	37

changes in lattice parameters with composition are governed by the relative sizes of the atoms or ions. According to Vegard's law, the linear increase of the lattice parameters with the radius of the alkaline-earth oxides would be expected for true solid solutions. In our case, the slight linear variation of Sm_2O_3 lattice parameter with the size of M^{2+} ions is indicative of the fact that the miscibility of component oxides existed but, was relatively limited (see inset in Fig. 1 and comparison with the standard pure Sm_2O_3 phase $a = 10.927$ Å). This fact is confirmed by the XPS investigation of the surface composition. Very weak XRD lines of alkaline-earth/zinc oxides could be also identified. The absence of intense and well-defined XRD characteristic reflections of alkaline-earth oxides/ZnO can be explained by the limitations of XRD method. The sensitivity is not high enough to identify low amounts of crystalline phases or small crystalline domains. In the case of the of the MgO–Sm_2O_3 sample, the crystallization degree of cubic crystalline Sm_2O_3-phase is lower and crystallize along with a phase exhibiting very broad peaks. Considering the overlapping effect of the peak positions due to the quasi-amorphous characteristic of the phase (low crystalline dimensions and defects) the phase could be monoclinic Sm_2O_3 (JCPDS file 43-1030). Small amount of $SrCO_3$ phase was also present in XRD pattern. In fact our sample consisted of a combination of solid solution and segregated oxide phases. In our view, for catalytic processes is important to have a good correlation between catalytic behavior and surface composition data to help the interpretation of experimental data.

3.2. Catalytic test

The catalytic behavior of the investigated mixed oxides, expressed in terms of methane conversion, reaction selectivity and yield to C_2^+ and the level (concentration) of CO_2, is presented in Fig. 2. In all cases, $X(CH_4)$, $S(C_2^+)$ and $Y(C_2^+)$ showed a progressive increase with increasing reaction temperature up to a maximum located between 775 and 800 °C. For T >775–800 °C the reaction selectivity and yield to C_2^+decreased, most likely because of kinetic limitations. The upper limit of OCM yield under conventional packed bed, continuous feed reactor is considered to be governed by the enthalpies of hydrogen abstraction from CH_4 and oxygen dissociative adsorption [1]. By this procedure limit of 28% for C_2^+ yield was determined for a continuous CH_4/O_2 co-fed, single pass process under conventional conditions used for catalyst screening. As can be seen in Fig. 2, the order of catalytic activity for hydrocarbon production at 775 °C was Sr > Ca > Mg > Zn. $SrCO_3$ was already reported to be a good promoter enhancing the catalytic activity of Sm_2O_3 for C_2^+ production [3]. The values for C_2^+ yields [$Y(C_2^+)$], methane conversion [$X(CH_4)$], selectivity for hydrocarbon formation [$S(C_2^+)$], determined at the peak catalytic activity at 775 °C, are presented in Table 3. The surface areas of the as prepared mixed oxide, listed in Table 3, ranged between 6 and 11.3 $m^2\,g^{-1}$. These low surface areas, typical for most of the OCM catalysts, seems not having a determinant influence on the catalytic behavior. The unselective reaction product of methane oxidative conversion in OCM reaction is CO_2. The mechanism of CO_2 formation was analyzed by several isotope-exchange as well as by kinetic studies [4]. The aim was to get a better understanding on the mechanism of CO_2 formation and thus to find practical ways to decrease the activity of the sites responsible for CO_2 production. Thus, it is useful to compare the CO_2 levels in the mixtures of reaction products with the basicity of mixed oxides. Fig. 2 presents comparatively methane conversion over MO–Sm_2O_3 (M = Zn, Mg, Ca, Sr) oxides as a function of reaction temperature. Over the investigated mixed oxides, CO_2 showed a general tendency to slightly decrease with reaction temperatures. The formation of CO_2 takes place at the lowest OCM reaction temperatures by consuming most of the oxygen contained in reaction mixture. The concentration of CO_2 afterwards decreases slowly with temperature as the formation of C_2^+ hydrocarbons becomes favored. On the other hand, the average amount of produced CO_2 is clearly related to the overall basicity of oxide catalysts. The combination of lower basicity oxides (ZnO or MgO) with Sm_2O_3 favored the formation of larger amounts of CO_2 over the temperature range investigated whereas on the mixed oxides possessing higher alkalinity (CaO–Sm_2O_3 and SrO–Sm_2O_3) the formation of CO_2 was hindered. The order of activity for CO_2 production in the 550–820 °C temperature range was ZnO–Sm_2O_3 > MgO–Sm_2O_3 > CaO–Sm_2O_3 ≅ SrO–Sm_2O_3. Wang et al. [5] pointed out that basic catalysts are effective for C_2^+ production but on the other hand they are also extensively poisoned by gas phase CO_2. The impact of gas phase CO_2 on the catalytic behavior, via the formation of surface carbonate species, was additionally suggested by transient isotope exchange studies [6]. The effect of CO_2 on $Y(C_2^+)$ was investigated for several alkaline and alkaline-earth elements by Suzuki et al. [7]. With CO_2 as diluent, the C_2^+ yield and selectivity increased for MgO. With CaO catalyst, a positive effect on C_2^+ formation was observed only at low CO_2 partial pressures whereas in the case of SrO, the CO_2 completely suppressed the catalytic activity for OCM reaction. The conclusion was that the deactivation was caused by the formation of highly stable carbonate species on the surface of oxide catalysts. The kinetic investigation of Roos et al. [8] concluded also that carbon dioxide acts as a poison for the coupling reaction and this effect should be taken into account in the kinetic evaluation of catalytic behavior. A quantitative relationship between the catalytic activity for C_2^+ production and the concentration of surface basic sites interacting with the CO_2 was demonstrated for the first time in a recently published work [2]. Based on the above considerations, we have tried to take a look on the relationship between thermal decomposition of surface carbonate species of MO–Sm_2O_3 mixed oxides and the generation of basic active sites.

3.3. Basicity investigation by TPD

The first step of the investigation aimed to prove that the efficiency of C_2^+ formation at a given temperature is directly related to the available basic sites. The amount of surface carbonate species susceptible to decompose in reaction conditions were determined by quantitatively measuring the evolved CO_2. Then, the results were correlated with activity data. The acidic CO_2 is often used as probe molecule to measure the surface basicity. Acidity and basicity depend on the nature of oxide and on the charge and radius of metal ions. The surface species formed by different ways of CO_2 adsorption on the surface of oxides are hydrogencarbonyl ions, bi- and mono-dentate carbonate, and surface carbonyl [9]. In our specific case, the TPD of CO_2 was useful to provide information on the strength distribution of basic sites as well as allowed the quantitative measurement of basic sites formed by carbonate decomposition. The mixed oxides for TPD measurements were the spent catalysts used in OCM reaction up to 820 °C. The spent catalysts were cooled down slowly (10 °C min^{-1}) from the highest reaction temperature (850 °C) in reaction mixture to allow the re-carbonatation process. Then the mixed oxides were transferred quickly to the TPD measurement cell. The surface carbonate build-up and the decomposition process are controlled by the

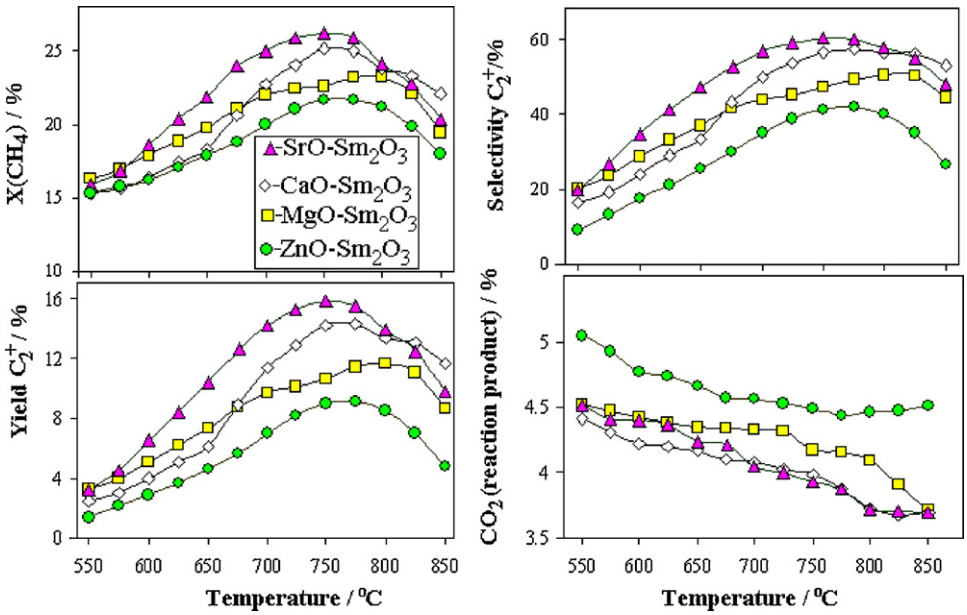

Fig. 2. Comparative methane conversion [$X(CH_4)$], selectivity to C_2^+, yield to C_2^+ and CO_2 production over $MO–Sm_2O_3$ (M = Zn, Mg, Ca, Sr) oxides as a function of temperature of OCM reaction.

thermodynamic equilibrium established at a given temperature in reaction conditions. As the reaction temperature increases, CO_2 is released progressively according to the strength of basic sites. Prior the TPD measurements, the mixed oxides were kept in pure Ar at 300 °C for 1 h to eliminate the weakly adsorbed CO_2. Thus, it is expected to measure only the CO_2 directly bound to the basic sites of mixed oxides. It should be mentioned that the amounts of surface carbonate for all investigated samples were reproducible within a margin error of ±10%. In mean time, the shapes of TPD spectra were similar proving that the number, nature and strength of basic sites were preserved after two successive catalytic runs.

The comparative TPD profiles of spent catalysts are shown in Fig. 3. The CO_2 desorption peaks observed for $ZnO–Sm_2O_3$ (at 510 and 609 °C), $MgO–Sm_2O_3$ (at 580 and 656 °C) and $SrO–Sm_2O_3$ (at 656 and >800 °C) are consistent with different types CO_2 retained by the alkaline sites of mixed oxides. In other words, not all the basic sites of the investigated mixed oxides are equivalent. There is a distribution of basic sites strength and this is reflected in the ability to bind CO_2. In the case of $CaO–Sm_2O_3$, only one large desorption peak could be observed at 656 °C. The second observation is that, the CO_2 desorption maxima are shifted to higher temperatures with the increase in MO basicity: ZnO ≅ MgO < CaO < SrO. There is a direct relationship between the binding strength of CO_2 species and the basicity of MO oxides contained by the $MO–Sm_2O_3$ mixed oxides. The more basic are the basic sites the higher is the temperature at which CO_2 is released. It should be emphasized that the surface carbonate species are regenerated in the lower temperature domain during the cooling process. The quantities of desorbed

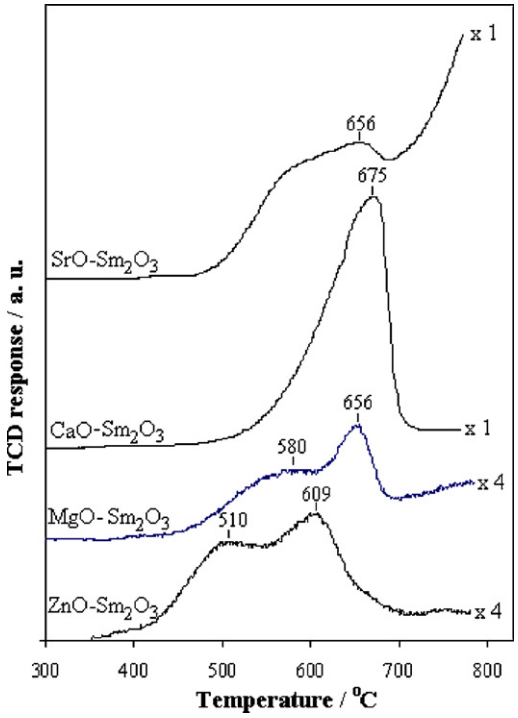

Fig. 3. TPD spectra of CO_2 evolved from $MO–Sm_2O_3$ (M = Zn, Mg, Ca, Sr) oxide catalysts used in OCM reaction.

Table 3
Characterization data and catalytic activity of $MO–Sm_2O_3$ mixed oxides for OCM reaction.

Catalysts	[a]$X(CH_4)$/%	[a]$S(C_2^+)$/%	[a]$Y(C_2^+)$/%	[b]Suface carbonate/mmol g_{cat}^{-1}	$S_{BET}/m^2\ g^{-1}$	[c]$r(C_2^+)$/mol s^{-1} g_{cat}^{-1}	[d]TOF $(C_2^+)/s^{-1}$
$ZnO–Sm_2O_3$	21.7	41.9	9.1	0.58	6.8	2.6×10^{-5}	0.04
$MgO–Sm_2O_3$	23.2	49.2	11.4	0.53	11.3	3.4×10^{-5}	0.06
$CaO–Sm_2O_3$	25.0	57.2	14.3	2.38	6.0	4.4×10^{-5}	0.02
$SrO–Sm_2O_3$	25.9	59.8	15.5	2.81	6.4	5.0×10^{-5}	0.02

[a] The catalytic activity data measured at 775 °C.
[b] Amount of surface carbonate formed in reaction conditions.
[c] $r(C_2^+)$ represents the rate of C_2^+ formation.
[d] $TOF(C_2^+)$ represents the turnover frequency of C_2^+ formation over the alkaline sites of mixed-oxide catalysts.

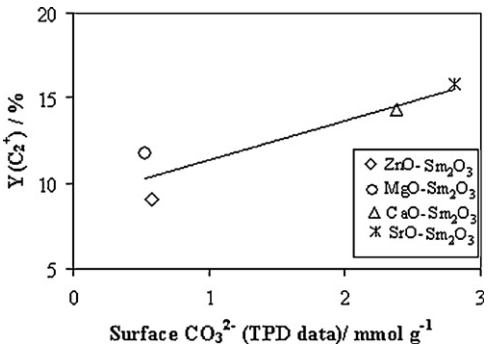

Fig. 4. Relationship between the peak yields to C_2^+ and amount of surface carbonate determined quantitatively from TPD data.

CO_2, calculated by integrating the surface area under TPD curves represented in Fig. 3, are listed in Table 3. The total amounts of desorbed CO_2 up to 800 °C, reflecting the basicity of the MO oxides were 0.58 mmol g^{-1} for $ZnO–Sm_2O_3$, 0.53 mmol g^{-1} for $MgO–Sm_2O_3$, 2.38 mmol g^{-1} for $CaO–Sm_2O_3$ and 2.81 mmol g^{-1} for $SrO–Sm_2O_3$. The slightly higher basicity of ZnO (0.58 mmol g^{-1}) compared to MgO (0.53 mmol g^{-1}), is in agreements with previously published microcalorimetric studies [9]. In contrast to MgO, which is practically free of acid sites, ZnO possess larger amount of acid sites compared to the basic one. Strong and weak acid sites have been identified on ZnO by using ammonia adsorption [10]. As we shall show later, the acid sites of ZnO enhanced the production of CO_2, decreasing thus the reaction yield to C_2^+. The total number of basic sites reported for $CaO–CeO_2$ mixed oxides, measured by TPD of CO_2, ranged between 0.4 and 0.7 mmol g^{-1} [11]. In contrast to other samples, the evolvement of CO_2 from $SrO–Sm_2O_3$ is not a completed process up to 800 °C, meaning that significant amount of carbonate remained on the surface at the end of TPD runs. The activity of $SrO–Sm_2O_3$ is hindered to some extent because the strong basic sites (supposed to exhibit high catalytic activity) are unavailable to reactants because they are blocked by CO_2. However, the total number of available basic sites of $SrO–Sm_2O_3$ (2.81 mmol g_{cat}^{-1}) at peak activity temperature (775 °C) is higher compared to the other mixed oxides. The published studies devoted to the investigation of oxide basicity by using the TPD of low-temperature adsorbed CO_2 are not always fully relevant because the surface of strong basic oxides are already in most cases covered by very stable carbonate species. Greis [12] suggested that, to completely remove all the carbonate contaminants of hexagonal rare-earth oxides, temperatures between 1000 and 1600 °C had to be employed. Therefore, pretreatment at high temperature is absolutely necessary to obtain carbonate-free oxide surfaces. The calcination temperature of SrO should be higher than 1000 °C to decompose the surface carbonate species. Our results lead to the idea that the catalytic activity for C_2^+ formation can be correlated to the total number of available basic sites (free of CO_2). Our approach was to measure the amount of CO_2 originating from the decomposition of already existing surface carbonate which was formed in reaction condition. Thus, the concentration of basic active sites formed by the elimination of CO_2 can be accurately measured and then correlated with the catalytic activity for C_2^+ formation.

The relationship between the amount surface carbonate decomposed in the 350–820 °C temperature range, determined by measuring the released CO_2, and the catalytic activity for C_2^+ production is presented in Fig. 4. The data plotted in Fig. 4 suggest a close relationship between the number of available basic sites and the reaction yield to C_2^+. The OCM reaction yield to C_2^+ is proportional to the number of available basic sites in reaction conditions.

Table 4
Atomic composition on surface of $MO–Sm_2O_3$ (M = Zn, Mg, Ca, Sr) determined from XPS data.

Catalyst	Surface composition (at.%)				
	Sm (3d5/2)[a]	M[b]	O[c]	O(CO_3^{2-})[d]	C(CO_3^{2-})[e]
$ZnO–Sm_2O_3$	36.2	4.8	11.5	32.6	11.1
$MgO–Sm_2O_3$	34.9	4.4	14.6	30.9	10.8
$CaO–Sm_2O_3$	27.8	4.6	6.6	40.8	16.9
$SrO–Sm_2O_3$	30.7	8.4	6.1	37.2	15.1

[a] 3d5/2 line BE at ≅1083 eV.
[b] M = Zn (2p3/2 line BE at 1022.3 eV), Mg (2p line BE at 50.2 eV), Ca (2p3/2 line BE at 346.6 eV), Sr (3d5/2 line BE at 133.5 eV);.
[c] O(1s) line BE at 529 eV characteristic for surface bound oxygen species.
[d] O(1s) line BE at 532 eV characteristic for oxygen contained in CO_3^{2-}.
[e] C(1s) line BE at 289.7 eV, characteristic for carbon contained in CO_3^{2-}.

3.4. XPS analysis

The surface basicity, responsible for catalytic behavior, may not necessarily reflect the bulk composition of mixed oxides. In this context, the catalytic properties are particularly sensitive to preparation conditions [13] as well as to the precursor used [14]. Thus, the surface composition of the catalytic materials has been also investigated by XPS. The C 1s binding energy peak at 285.0 eV was used as standard for internal calibration. The peak at 289.6 eV, observed at all samples, is attributable to the surface carbonates. The atom percentages of the elements were calculated from the peak normalized areas. The atomic sensitivity factors were derived from the electronic cross-section of each element using the transmission and inelastic mean free path corrections. The weight fractions of various elements were then determined taking into account the atomic mass of each element.

The results presented in Table 4 show that MO oxides tend to accumulate on the surface as the enthalpy for carbonate formation increases. On the other hand, the enthalpy for carbonate formation is directly related to the oxides basicity. The increase in the surface concentration of alkaline-earth elements is reflected also the enhancement of catalytic activity for C_2^+ production (see Figs. 2 and 4).

The surface bound oxygen species give characteristic binding energies at ≈529 eV. The oxygen of surface carbonates is characterized by higher binding energies, at around 532 eV (see Fig. 5). These assignments are in agreement with the electron spectroscopy study of Voights et al. [15] investigating the formation of carbonate on CaO films. The formation mechanism consists in the adsorption of CO_2 on lattice O^{2-} sites along with the bending of O–C–O bonds. This very fast process is restricted to the top surface layer. The assignments of the binding energies for the prominent transitions of Ca, Mg, Sr and Zn are presented in Table 4. In the case of samarium, the $3d_{5/2}$ binding energy of 1083.3 ± 0.1 eV is characteristic for Sm^{3+} oxide. The position of Sm $3d_{5/2}$ binding energy was not affected by the amount of surface carbonate. Thus, MO oxides seem to be mostly responsible for the generation of surface carbonate species. The contribution of samaria to the formation of basic sites cannot be ruled out but the effect on XPS spectra are negligible. In other words, the difference between $Sm^{3+}–O^{2-}$ and $Sm^{3+}–CO_3^{2-}$ binding energy energies are below the detection limit of XPS method [16].

According to the XPS data presented in Fig. 6, the mixed oxides show an increasing tendency for surface carbonate formation in the order Zn ≈ Mg < Ca < Sr. This situation is in agreement with order of basicity strength within the series of alkaline-earth oxides and with CO_2 TPD data. In addition, the relative concentration of carbon belonging to surface carbonate increases also in the same manner confirming the close relationship existing between the equilibrium amount of surface carbonate formed in reaction conditions and

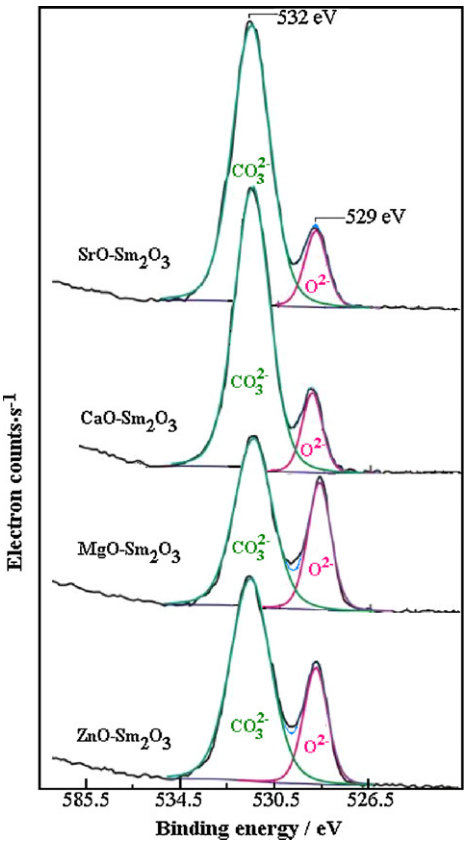

Fig. 5. Comparative presentation of the relative amounts of bound oxygen and oxygen contained in carbonate species (CO_3^{2-}) on the surface of MO–Sm_2O_3 mixed oxides (M = Zn, Mg, Ca, Sr).

overall basicity of mixed-oxide catalysts. On the other hand, Fig. 7 reveals that the relative concentration of surface bound oxygen controls the reaction selectivity for CO_2. Thus, the surface bound oxygen seems to be the sites involved in the unselective oxidation of methane to CO_2.

3.5. FTIR analysis

The surface carbonate species formed on the surface of MO–Sm_2O_3 mixed oxides were investigated by IR spectroscopy. Fig. 8 presents the IR spectra of the mixed oxides used in OCM reaction followed by post conditioning in Ar at 350 °C for 1 h to eliminate the physisorbed CO_2. IR bands characteristic for different types of surface carbonate species could be identified in the

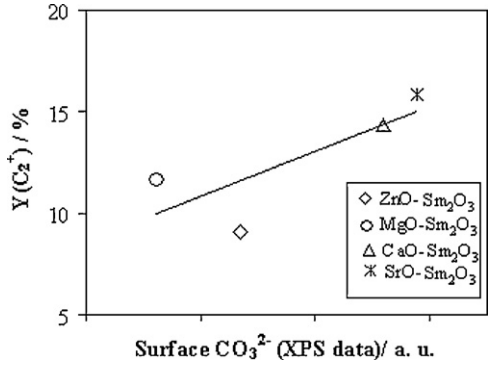

Fig. 6. Relationship between the amounts of surface carbonate estimated from XPS data (electron counts of oxygen in CO_3^{2-} species) and catalytic peak activity for C_2^+ formation over MO–Sm_2O_3 mixed oxides.

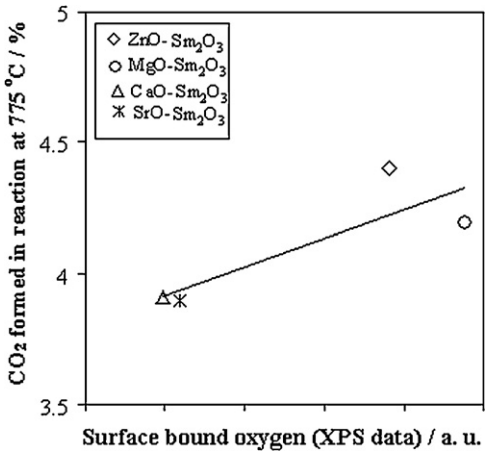

Fig. 7. Relationship between the amounts of surface bound oxygen derived from XPS data and catalytic activity for CO_2 formation over MO–Sm_2O_3 mixed oxides at 775 °C.

1395–1654 cm^{-1} region for all the investigated oxides. The IR spectra revealed the existence of two species having different energies. Generally, the stronger bounded mode can be assigned to the monodentate carbonate and the weaker one to the bidentate carbonate [9].

The IR bands of interest for ZnO–Sm_2O_3 are located at 1395 and 1520 cm^{-1}, and these bands are attributable to the monodentate carbonate species [17,18]. From here comes out that, the carbonate is formed on preferentially on the alkaline sites of ZnO.

In the case of MgO–Sm_2O_3, three characteristic IR band have been observed at 1416, 1544 and 1654 cm^{-1}. On simple MgO, the characteristic IR bands at 1390 and 1520 cm^{-1} have been attributed to the unidentate CO_2 whereas the bidentate carbonate species are characterized by an IR band at 1670 cm^{-1} [19]. Thus, the IR bands detected on MgO–Sm_2O_3 at 1416 and 1544 cm^{-1} can be assigned

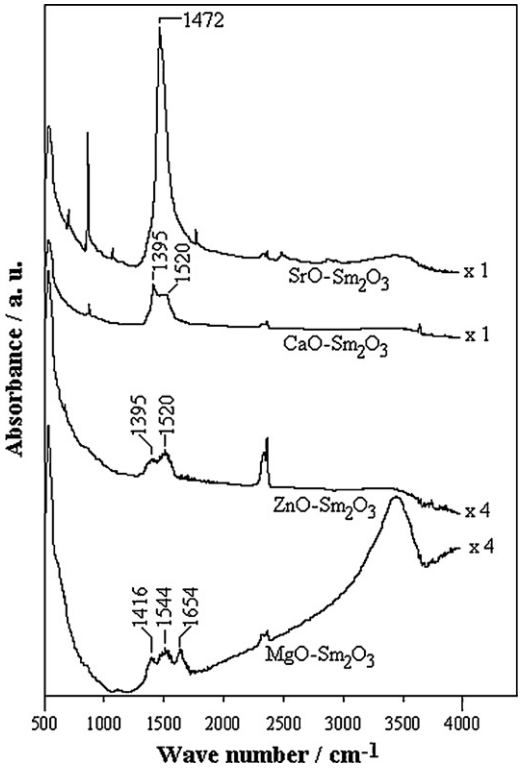

Fig. 8. Comparative IR spectra of the MO–Sm_2O_3 oxides (M = Zn, Mg, Ca and Sr).

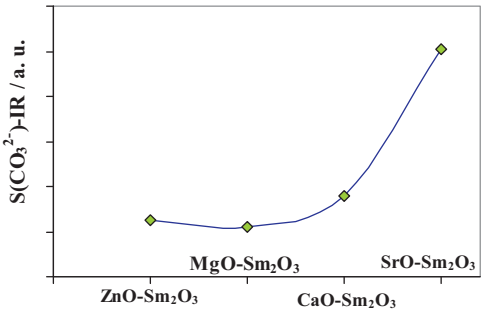

Fig. 9. Surface basicity evaluated from the integrated area of ν_{CO2} band in the 1395–1654 cm^{-1} region.

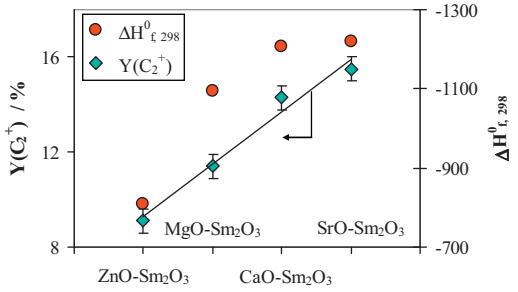

Fig. 10. Comparative plots of MCO_3 carbonate formation enthalpy and C_2^+ yields over MO–Sm_2O_3 mixed oxides (M = Zn, Mg, Ca, Sr).

to the unidentate CO_2 whereas the band at 1654 cm^{-1} to the bidentate CO_2. It can be assumed that the surface carbonate species are related to the basic sites of MgO, probably the low coordinated O^{2-} sites located at corners or edges [20]. These sites can adsorb CO_2 more strongly than the highly coordinated O^{2-} ions located on planes.

The IR bands of interest for CaO–Sm_2O_3 at 1395 and 1520 cm^{-1} can be attributed in this case to the vibration of unidentate CO_2 on the alkaline sites of CaO.

SrO–Sm_2O_3 sample shows only one broad IR band with the maxima at 1472 cm^{-1}. This broad IR band may contain the characteristic vibration of both, monodentate and bidentate carbonates. The main IR bands of carbonate species on SrF_2/Nd_2O_3 surface were observed at 1420 and 1520 cm^{-1} [21]. From the surface area of the IR peak attributable to carbonate species in Fig. 9, it can be said that the largest amount of carbonate is formed on SrO–Sm_2O_3. The plot of Fig. 9, correlating well with XPS (Table 4) and TPD (Fig. 3) results, suggests that the mixed oxide containing ZnO exhibits higher affinity for CO_2 compared to MgO.

According to IR results, (i) monodentate as well as bidentate carbonate species are formed on the surface of MO–Sm_2O_3 mixed oxides, (ii) MO oxides are mostly responsible for the formation of surface carbonate species and (iii) the amount of surface carbonate of mixed oxides correlates well with the basicity of MO oxides.

Fig. 10 presents comparatively the yield to C_2^+ over MO–Sm_2O_3 mixed oxides and the carbonate formation standard enthalpy ($\Delta H^\circ_{f,298}$) for MO oxides. The enthalpy for MCO_3 formation reflects in fact the basicity of MO. Thus, the plots represented in Fig. 10, suggests that the stronger the basicity of MO is the higher is the activity of MO–Sm_2O_3 for C_2^+ formation. The relationship between $\Delta H^\circ_{f,298}$ and $Y(C_2^+)$ is not strictly linear because the catalytic activity is mainly related to the amount and distribution of basic sites on the surface.

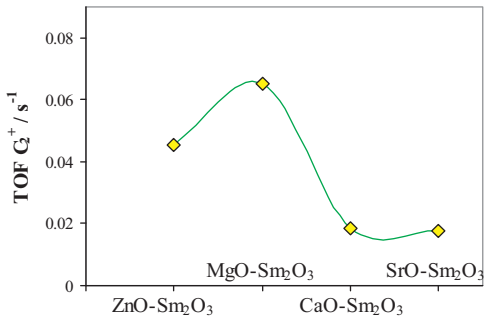

Fig. 11. Dependence of TOF values for C_2^+ formation on the nature of MO metal oxides (M = Zn, Mg, Ca and Sr) added with samaria.

3.6. TOF estimation

The TOF (turnover frequency) values for C_2^+ formation at 775 °C over the investigated mixed oxides are presented in Fig. 11. The TOF values were calculated by dividing the experimentally measured reaction rates (see Table 3) to the total number of basic sites responsible for C_2^+ formation. The total number of basic sites was determined from the amount of desorbed CO_2 and their values are also listed in Table 3 as quantity of surface removable carbonate. Studies reporting on the determination of TOF values for hydrocarbon oxidation on metal oxides are very scarce. The main difficulties consisted in the identification of active sites and in finding reliable experimental methods for measuring their concentration. A recently published work established for the first time a methodology for the identification of the active sites formed under reaction conditions, making thus possible the calculation of TOF values over MO–Nd_2O_3 (M = Be, Mg, Ca and Sr) mixed oxides [2]. The TOF values determined for BeO–Nd_2O_3, MgO–Nd_2O_3, CaO–Nd_2O_3, SrO–Nd_2O_3 at 775 °C were 0.12, 0.04, 0.02 and 0.03 s^{-1}. These values are very close or even similar (in the case of calcium) for the corresponding alkaline-earth element to those presented in Table 3. It comes out that, the contribution of the rare earth element to the overall catalytic is either limited or relatively constant regardless the nature of rare-earth element. The rare-earth elements act as an effective dispersing matrix for the catalytically active basic oxides of MO. According to the XPS results presented in Table 4, the surface is enriched in Sm_2O_3 compared to MO. The average atomic ratio between Sm and M is 1 to 8.

High alkaline site concentration of CaO–Sm_2O_3 and SrO–Sm_2O_3 gave lower TOF values for C_2^+ formation. The relation between overall activity and TOF is not very clear at this stage. In fact, the basic sites used in our calculations are not equivalent and there is a distribution of their strength. The optimum basicity for OCM reaction should be determined to have a good correlation between catalytic activity and TOF. Actually, the TOF values reflect only the relationship between activity and total number of basic sites and not the specific contribution of each type of basic sites to the overall activity. This may explain the apparent contradiction between basicity, catalytic activity and TOF values. Interesting beneficial synergetic effects have been reported for mixtures of rare earth oxides [22]. The synergetic effect taking place between the alkaline-earth oxides and rare earth oxides, which may a factor mediating the complex relationship between the concentration and strength of alkaline active sites, is currently under a detailed investigation.

3.7. Impact of acid-basic properties on catalytic behavior

The summary of our results is schematically presented in Fig. 12. A parallel reaction pathway was already suggested by Parida and Rao [23]. Our experimental results support also the idea that

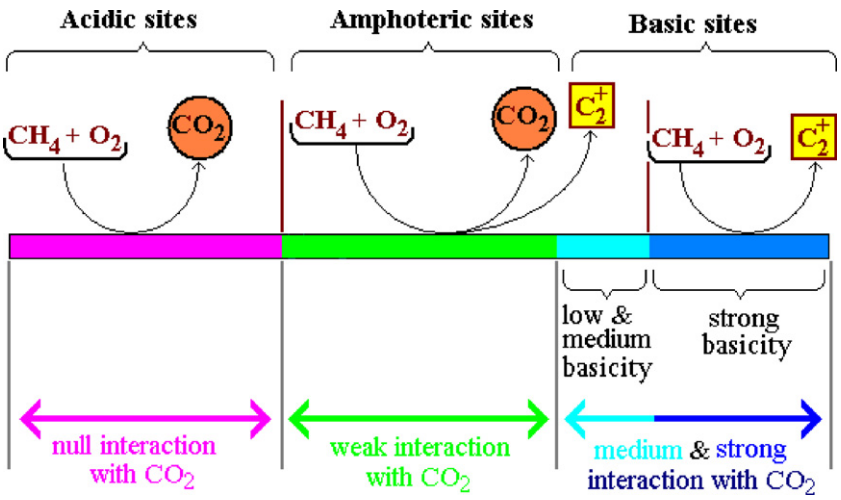

Fig. 12. Schematic behavior of mixed oxide catalysts in OCM reaction as a function of their acid–base properties.

methane is converted to products by independent pathways on two types of active sites. The alkaline active sites, which are inactive at low temperatures because they are blocked by CO_2, are responsible for selective C_2^+ formation. By increasing the reaction temperature, the active sites start to be progressively available for methane activation due to CO_2 desorption. The concentration of free basic sites at a given reaction temperature is controlled by the thermal stability of surface carbonate. It is generally accepted that methane conversion to C_2^+ implies the $H^\bullet$ extraction by the basic site of oxide catalysts and the generation of $CH_3^\bullet$ radicals which are undergoing to coupling in gas phase to generate C_2H_6. The basic sites can be all the aforementioned oxygen species (O^-, O_2^- and O_2^{2-}) identified in previous studies [24]. These sites should have the essential feature to give electrons or ability to share an electron pair. The basic sites are often reported to be surface defects. Some relevant examples are the generation of Li^+O^- pair defects by doping MgO with Li^+ [25] and basic lattice defects creation (i.e. oxygen vacancies) by dispersing La^{3+} in CeO_2 matrix [26]. The alkaline doping creates surface basic sites of different types and strength. It should be mentioned that the basic strength is likely to depend on other additional factors, such as location on the surface (edges, kinks, corners, etc.) [20]. Debates on the reaction mechanism are still going on. The main goal of our work was to correlate in a systematic way the activity with acid–base property of the mixed oxide catalysts. The most important feature of active centers for OCM reaction is that they posses basicity, and this property is the relevant one in OCM reaction. The availability to reactants and activity of basic sites in reaction conditions are very different compared to acid sites.

The formation of CO_2 reaction product takes place on acid type as well as on amphoteric sites showing low affinity for CO_2. Thus the production of CO_2, starting at low temperatures, shows little dependency on reaction temperature. The nature of sites responsible for methane total oxidation was assumed to be acidic [27]. According to isotope-exchange studies, the formation of CO_2 takes place via multistep surface oxidation mechanism [28]. This reaction mechanism is confirmed also by other studies observing that CO_2 is not formed in gas phase but on the catalyst surface [29]. In addition to the published results, our XPS data confirm that the concentration of acid sites increases as the overall basicity of the mixed oxides decreases. These sites are fully available and active to convert CH_4 and O_2 reactants to CO_2 and H_2O starting from reaction temperatures as low as 350 °C. Therefore, methane is combusted to CO_2 by completely consuming oxygen contained by reaction mixture up to 550 °C (see Fig. 2). As the reaction temperature increases, the CO_2 is progressively desorbed and the formation of C_2^+ is taking place along with CO_2. The basic sites in this stage are still poisoned by a strongly adsorbed CO_2 (stable carbonate). By further raising temperature, the strong basic sites become available by decomposition of surface carbonate. It was reported that very strong basic sites are detrimental to OCM reaction because the strong adsorption of CO_2 is blocking these sites [11]. On basic sites methane is selectively activated to $CH_3^\bullet$ radicals. Further, the gas phase coupling of methyl radicals lead to the formation of C_2^+.

In an attempt to prove the validity of our theory and to demonstrate that only the acid sites of the mixed oxide are responsible for CO_2 production, to the initial reaction mixture (CH_4 and O_2) was added 6% NH_3. The selected mixed oxide for this experiment was SrO–Sm_2O_3, showing the best catalytic performances for OCM reaction among the investigated mixed oxides. The aim was to hinder the formation of CO_2 by poisoning selectively acid sites with NH_3. The observed results were quite suggestive. The formation of CO_2 was completely hindered in the presence of basic ammonia. The only product of methane unselective oxidation was CO. The concentration of CO was around 80% of that of CO_2 in the 550–850 °C temperature range. In addition, in the presence of NH_3, methane conversion decreased by ≈30%, the concentration of C_2^+ (ethane + ethylene) decreased by 34%, the selectivity to C_2^+ remained relatively unchanged and corresponding reaction yield to C_2^+ decreased by 39%. The preliminary conclusion of this catalytic test is that, NH_3 depressed the activity of acid sites responsible for total oxidation of methane as the only oxidation product was CO. On the other hand, the decrease in catalyst oxidation capacity was associated with a decrease in methane conversion affecting thus the reaction yield to C_2^+. A general conclusion from this experiment is difficult to draw at this stage. However, it seems that the basic NH_3 interacted not only with the acidic sites of SrO–Sm_2O_3 but also with sites (probably amphoteric or slightly basic) contributing to the formation of C_2^+. It is clear that the basicity of poisoning molecule should be tuned properly to maximize the production of C_2^+ and to minimize the formation of CO_x.

4. Conclusions

The behavior in OCM reaction of catalytic oxide materials can be interpreted in term of solid acid–base catalysis. A correlation between the catalytic activity and the strength and number of basic sites was revealed.

The experimental results confirmed the idea that methane is converted to products on two types of active sites via independent pathways. The formation of CO_2 reaction product takes place on acidic sites. These sites show little interaction with gas phase CO_2. On the other hand, the catalytic behavior of acidic sites for methane combustion can be altered by basic molecules such as NH_3. The formation of C_2^+ takes place only when the reaction temperature is high enough ($T > 500\,^{\circ}C$) to trigger the removal of CO_2 adsorbed on the basic sites of oxides. The progressive increase of the number of available alkaline active sites by decomposition of surface carbonate species correlates well with the activity for the formation of C_2^+. There is a complex relationship between concentration, strength of alkaline active sites and TOF for C_2^+ production. In light of the experimental results, a strategy for improving the performances of OCM catalysts must take into consideration the identification of molecules with optimum basicity to selectively poison the acidic sites responsible for methane unselective oxidation. Another possibility is to find suitable preparative methods to poison or to reduce the number of surface acid sites.

References

[1] Y.S. Su, J.Y. Ying, W.H. Green Jr., J. Catal. 218 (2003) 321–333.
[2] F. Papa, D. Gingasu, L. Patron, A. Miyazaki, I. Balint, Appl. Catal. A 375 (2010) 172–178.
[3] K. Wang, S. Ji, X. Shi, J. Tang, Catal. Commun. 10 (2009) 807–810.
[4] K.P. Peil, J.G. Goodwin, G. Marcelin, J. Phys. Chem. 93 (1989) 5977–5979.
[5] D. Wang, M.P. Rosynek, J.H. Lunsford, J. Catal. 151 (1995) 155–167.
[6] A. Burrows, C.J. Kiely, G.J. Hutchins, R.W. Joyner, M.Y. Sinev, J. Catal. 167 (1997) 77–91.
[7] T. Suzuki, K. Wada, Y. Watanabe, Appl. Catal. 59 (1990) 213–225.
[8] J.A. Roos, S.J. Korf, R.H.J. Veehof, J.G. Van Ommen, J.R.H. Ross, Appl. Catal. 52 (1989) 131–145.
[9] A. Auroux, A. Gervasini, J. Phys. Chem. 94 (1990) 6371–6379.
[10] S.P. Naik, J.B. Fernandes, Thermochim. Acta 332 (1999) 21–25.
[11] Istadi, N.A.S. Amin, J. Mol. Catal. 259 (2006) 61–66.
[12] O. Greis, J. Solid State Chem. 34 (1980) 39–44.
[13] J.A.S.P. Carreiro, M. Baerns, J. Catal. 117 (1989) 258–265.
[14] V.R. Choudhary, V.H. Rane, R.V. Gadre, J. Catal. 145 (1994) 300–311.
[15] F. Voights, F. Bebensee, S. Dahle, K. Volgmann, W. Maus-Friedrichs, Surf. Sci. 603 (2009) 40–49.
[16] SNIST X-Ray Photoelectron Spectroscopy Database, Version 4.0, National Institute of Standards and Technology, Gaithersburg, 2008.
[17] G. Busca, V. Lorenzelli, Mater. Chem. 7 (1982) 89–126.
[18] G. Marbán, I. López, T. Valdés-Solis, Appl. Catal. A 361 (2009) 160–169.
[19] Y. Hao, M. Mihaylov, E. Ivanova, K. Hadjiivanov, H. Knözinger, B.C. Gates, J. Catal. 261 (2009) 137–149.
[20] M.-L. Bailly, C. Chizallet, G. Costentin, J.M. Krafft, H. Lauron-Pernot, M. Che, J. Catal. 235 (2005) 413–422.
[21] L.-H. Wang, X.-D. Yi, W.-Z. Weng, H.-L. Wan, Catal. Today 131 (2008) 135–139.
[22] A.G. Dedov, A.S. Loktev, I.I. Moiseev, A. Aboukais, J.-F. Lamonier, I.N. Filimonov, Appl. Catal. A 245 (2003) 209–220.
[23] K.M. Parida, S.B. Rao, React. Kinet. Catal. Lett. 44 (1981) 95–101.
[24] G.J. Hutchings, M.S. Scurrell, J.R. Woodhouse, Chem. Soc. Rev. 18 (1989) 251–283.
[25] D.J. Driscoll, W. Martir, J.-X. Wang, J.H. Lunsford, J. Am. Chem. Soc. 107 (1985) 58–63.
[26] S. Bernal, G. Blanco, A.El. Amarti, G. Cifredo, L. Fitian, A. Gatayries, J. Martin, J.M. Pintado, Surf. Interface Anal. 38 (2006) 229–233.
[27] J.M. DeBoy, R.F. Hicks, J. Chem. Soc. Chem. Commun. 14 (1988) 982–984.
[28] P.F. Nelson, C.A. Lukey, N.W. Cant, J. Catal. 120 (1989) 216–230.
[29] S. Ahmed, J.B. Moffat, Appl. Catal. 54 (1989) 241–255.